GENERAL ARTICLE

A nonsense mutation in *myelin protein zero* causes congenital hypomyelination neuropathy through altered P0 membrane targeting and gain of abnormal function

Pietro Fratta[1,2,*,†], Francesca Ornaghi[2,3,7,†], Gabriele Dati[2,†], Desirée Zambroni[2], Paola Saveri[2,4], Sophie Belin[6,7], Patrizia D'Adamo[2], Michael Shy[5], Angelo Quattrini[2], M. Laura Feltri[2,7] and Lawrence Wrabetz[2,7,*]

[1]UCL Institute of Neurology, Queen Square, London WC1N 3BG, UK, [2]IRCCS San Raffaele Scientific Institute, DIBIT, 20132 Milan, Italy, [3]SR-TIGET, 20132, Milan, Italy, [4]Unit of Rare Neurodegenerative and Neurometabolic Diseases, Department of Clinical Neurosciences, C. Besta Neurological Institute IRCCS Foundation, 20133, Milan, Italy, [5]Department of Neurology, University of Iowa, 52242, Iowa City, IA, USA, [6]Department of Neuroscience and Experimental Therapeutics, Albany Medical College Department of Neuroscience and Experimental Therapeutics, 12208, Albany, NY, USA and [7]Departments of Neurology and Biochemistry, Jacobs School of Medicine and Biomedical Sciences, Hunter James Kelly Research Institute, State University of New York at Buffalo, Buffalo, NY 14203, USA

*To whom correspondence should be addressed at: Lawrence Wrabetz, IRCCS San Raffaele Scientific Institute, DIBIT, 20132 Milan, Italy. Tel: +17168818913; Fax: +17168496651; Email: lwrabetz@buffalo.edu. UCL Pietro Fratta, Institute of Neurology, Queen Square, London WC1N 3BG, UK. Tel: +442034484112; Fax: +442034484114; Email: p.fratta@ucl.ac.uk

Abstract

Protein zero (P0) is the major structural protein in peripheral myelin, and mutations in the *Myelin Protein Zero* (*Mpz*) gene produce wide-ranging hereditary neuropathy phenotypes. To gain insight in the mechanisms underlying a particularly severe form, congenital hypomyelination (CH), we targeted mouse *Mpz* to encode P0Q215X, a nonsense mutation associated with the disease, that we show escapes nonsense mediated decay and is expressed in CH patient nerves. The knock-in mice express low levels of the resulting truncated protein, producing a milder phenotype when compared to patients, allowing to dissect the subtle pathogenic mechanisms occurring in otherwise very compromised peripheral myelin. We find that P0Q215X does not elicit an unfolded protein response, which is a key mechanism for other pathogenic *MPZ* mutations, but is instead in part aberrantly trafficked to non-myelin plasma membranes and induces defects in radial sorting of axons by Schwann cells. We show that the loss of the C-terminal Tyr-Ala-Met-Leu motif is responsible for P0 mislocalization, as its

addition is able to restore correct P0Q215X trafficking *in vitro*. Lastly, we show that P0Q215X acts through dose-dependent gain of abnormal function, as wild-type P0 is unable to rescue the hypomyelination phenotype. Collectively, these data indicate that alterations at the premyelinating stage, linked to altered targeting of P0, may be responsible for CH, and that different types of gain of abnormal function produce the diverse neuropathy phenotypes associated with *MPZ*, supporting future allele-specific therapeutic silencing strategies.

Introduction

Mutations in the *myelin protein zero* (*MPZ*) gene are a major cause of inherited neuropathy and can manifest in a wide range of clinical phenotypes, ranging from early-onset forms, as Dejerine–Sottas syndrome (DSS) and congenital hypomyelination (CH), to less severe, adult onset, Charcot–Marie–Tooth diseases (CMT) [18,23].

Protein zero (P0), encoded by the *MPZ* gene, is primarily expressed in Schwann cells (SCs) and is the major structural transmembrane protein in peripheral myelin. P0 plays a crucial role in myelin formation by compacting adjacent wraps of SC plasma membrane, through *in trans* homophilic adhesion of its extracellular domain [3,5,8,20]. To date there are over 100 mutations in *MPZ*, known to cause peripheral neuropathies in patients and, although most of them are located in the extracellular domain of P0, few mutations in the short cytoplasmic domain were also reported [2,23]. The intracellular tail of P0 has several putative functions including compacting the cytoplasmic apposition in myelin [14], modulating adhesion by the P0 ectodomain [24,25,28] and directing trafficking of P0 through the YAML motif [12].

We have previously shown that different *MPZ* mutations act through distinct pathogenic mechanisms [15,27]. To further our understanding of how *MPZ* mutations cause disease, we generated a mouse model carrying the MPZQ215X mutation, which should eliminate part of the cytoplasmic domain and causes the severe CH neuropathy [13,21,23]. Here we show that lack of the last 33 amino acids induces an altered trafficking of the protein to non-myelin plasma membranes and is associated with altered radial axonal sorting by SCs in the early phases of myelination. We demonstrate that *Mpz* Q215X acts through a dose-dependent, gain of abnormal function that cannot be rescued by supplementing normal P0, carrying important implications for therapeutic strategies.

Results

Q215X escapes NMD and Mpz$^{Q215X/+}$ mice express low levels of mutant P0

The CH-causative *MPZ* Q215X mutation induces a premature stop codon and, due to its location in the penultimate exon, has been predicted to escape nonsense mediated decay (NMD) [10,11]. We therefore first tested the expression of the mutant and wild-type (WT) *MPZ* alleles from a skin biopsy of a patient carrying this mutation and found equal expression levels of the two alleles, supporting the prediction that the mutation is not subject to NMD (Fig. 1A). To allow disease mechanism investigations, we generated knock-in mouse lines by homologous recombination in embryonic stem (ES) cells (Supplementary Material, Fig. S1). We generated ES cells carrying the Q215X mutation and two control lines (LoxPA3 and LoxPD1), where we inserted the WT sequence. Q215X heterozygous (*Mpz*$^{Q215X/+}$) and homozygous (*Mpz*$^{Q215X/Q215X}$) mice along with

LoxP controls (*Mpz*$^{LoxP/+}$ and *Mpz*$^{LoxP/LoxP}$) were all viable. The Q215X mutation is predicted to encode for a truncated P0, lacking 33 amino acids of its C-terminal intracellular domain. Western blot analysis on sciatic nerve (SN) protein extracts of P28 WT, *Mpz*$^{Q215X/+}$and *Mpz*$^{Q215X/Q215X}$ mice confirmed the mutation produces a smaller P0 with a molecular weight of ~24 kDa (Fig. 1B and F). Surprisingly, the amount of the mutated protein was strongly reduced relative to endogenous P0. We therefore tested the levels of *Mpz* RNA and observed a reduction to 25% of WT levels (Fig. 1D and E). The mouse Q215X transcript was not targeted by NMD (Supplementary Material, Fig. S2), as predicted from patient data that was previously mentioned, and the reduction in expression was present also in control lines carrying only the LoxP site (Fig. 1D and E). Importantly, although the presence of LoxP accounts for a reduction at the RNA level, the amount of truncated protein was reduced in Q215X homozygous nerves compared to equally expressing LoxP homozygous nerves, suggesting that the mutation affects the protein stability (Fig. 1F and G). Thus, the Q215X knock-in mouse generated a truncated protein that was expressed at low levels, probably due to the combined effect of the LoxP site at the transcriptional level and of the truncation at the protein level.

Mpz$^{Q215X/+}$ mice develop a neuropathy with radial sorting defects

Whilst the Q215X mutation in patients induces an early disease onset and severe clinical features, the *Mpz*$^{Q215X/+}$mice showed no gross phenotype compared to controls and did not reveal any external sign of peripheral neuropathy (gait difficulty, tremor, atrophy of the hind limb musculature). In order to assess whether the mutant P0Q215X induces nerve abnormalities, we analysed semi-thin sections (STSs) of P28 SNs from *Mpz*$^{Q215X/+}$ mice, which revealed a mild hypomyelination when compared to controls (Fig. 2A). G-ratio analysis to assess myelin thickness confirmed the hypomyelination in *Mpz*$^{Q215X/+}$ and showed that was similar to the hypomyelination seen in P0 heterozygous knockout (*Mpz*$^{+/-}$) mice, which served as control for reduced *Mpz* expression (G-ratio Q215X/+0.69, P0+/−0.7, WT 0.65; Fig. 2B).

In patients, the Q215X mutation causes a deficit during development; we thus focused our analysis in the first 2 weeks of postnatal life. At P11, we observed bundles of unsorted mixed caliber axons in *Mpz*$^{Q215X/+}$ nerves (Fig. 2C, arrowheads) and not in WT littermates or in *Mpz*$^{+/-}$ mice (Fig. 2C). Unsorted axons were significantly augmented in *Mpz*$^{Q215X/+}$ compared to both WT and *Mpz*$^{+/-}$ mice (Fig. 2D, E), and at P14, the radial sorting defect was not visible anymore (data not shown) indicating that the deficit in P11 *Mpz*$^{Q215X/+}$ mice is that of a delay in myelination. We tested whether this defect resulted in a neuromuscular deficit using the rotarod and grid-walking tests. *Mpz*$^{Q215X/+}$ P10 to P12 mice showed a significant reduction in motor coordination compared to controls, revealing that the transient defect in the process of myelination identified in P11 mice results in a developmental motor deficit (Fig. 2F). A similar impairment was also detected
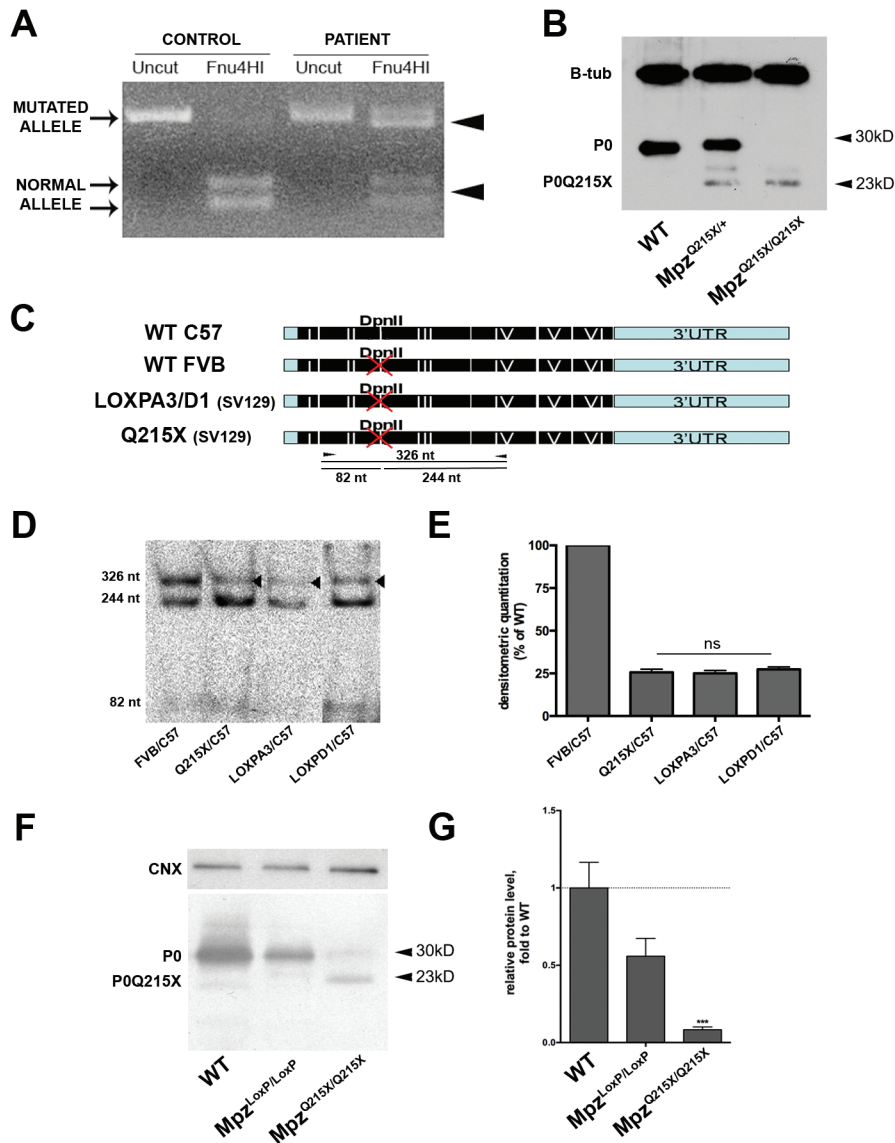
Figure 1. Q215X escapes NMD and Mpz$^{Q215X/+}$ mice express low levels of truncated protein. (**A**) Retrotranscribed and amplified *MPZ* RNA from a skin biopsy of a patient carrying the Q215X mutation shows similar expression of the mutated (uncut with Fnu4HI) and WT (cut) alleles. As expected, all transcripts are WT (cut) in a control sample. (**B**) Western blot using anti-P0 and anti-βTubulin on protein extracts from SNs of *Mpz*$^{+/+}$, *Mpz*$^{Q215X/+}$ and *Mpz*$^{Q215X/Q215X}$ sacrificed at postnatal day 28 show the presence of a truncated form of the protein at 23kD. (**C**) Schematic representation of the DpnII restriction enzyme sites in the different *Mpz* alleles. (**D**) DpnII restriction enzyme digestion of the retrotranscription (RT)-polymerase chain reaction (PCR)-amplified cDNA, obtained from RNA extracted from *Mpz*$^{+/+}$ (mice Friend Virus B mice (FVB)/C57Bl6), *Mpz*$^{Q215X/+}$ (129SVPas/C57Bl6) and two independent lines of *Mpz*$^{LoxP/+}$ (129SVPas/C57Bl6) P28 SNs. Given all targeted vectors were generated on 129SVPas background, and therefore did not carry the DpnII restriction site, we crossed all to C57Bl6 background, where the wt Mpz allele does have a DpnII restriction site. This allowed differentiation of WT *Mpz* (cut) and targeted alleles (uncut) by digestion. A WT mouse carrying one FVB allele (uncut) and C57Bl6 allele (cut) was used as technical control and showed equal amounts of expression from the two alleles. (**E**) Quantification of uncut band versus digested product (FVB WT transcript) are plotted showing a similar reduction in all samples carrying the LoxP site (*n* = 3 mice/genotype; one-way ANOVA, Tukey's post-test, *P*-value *ns* between samples carrying the LoxP site. Error bars represent SEM). (**F**) Anti-P0 western blot of protein extracts from *Mpz*$^{+/+}$, *Mpz*$^{LoxP/LoxP}$ and *Mpz*$^{Q215X/Q215X}$ p28 SNs. (**G**) Quantification of P0 normalized to calnexin is shown (*n* = 3 mice/genotype; two-way ANOVA, Bonferroni post-test, *P* < 0.001 versus WT. Error bars represent SEM).

using the grid walking test where P15 *Mpz*$^{Q215X/+}$ mice had a significantly higher number of errors compared to controls (analysis of variance [ANOVA] genotype effect $F[1,65] = 8.33$; $P = 0.005$, normalized on the same number of steps: ANOVA genotype effect $F[1,65] = 0.4$; $P = 0.52$) (Fig. 2G). These neuromuscular deficits are not present anymore in adult (P28) mice (data not shown). Taken together, these data show that the Q215X mutation, even expressed at low levels, induces an axonal radial sorting defect with delay in myelination leading to a dysmyelinating neuropathy. This early defect in postnatal life parallels the dysmyelinating disease reported for the two patients presenting Q215X *de novo* mutations and is specifically due to the presence of the Q215X-mutated glycoprotein and not to the lower expression of *Mpz*, as demonstrated by the absence of unsorted bundles of large caliber axons in P0+/− mice. These observations collectively suggest that Q215X acts via a gain-of-function (GOF) mechanism.
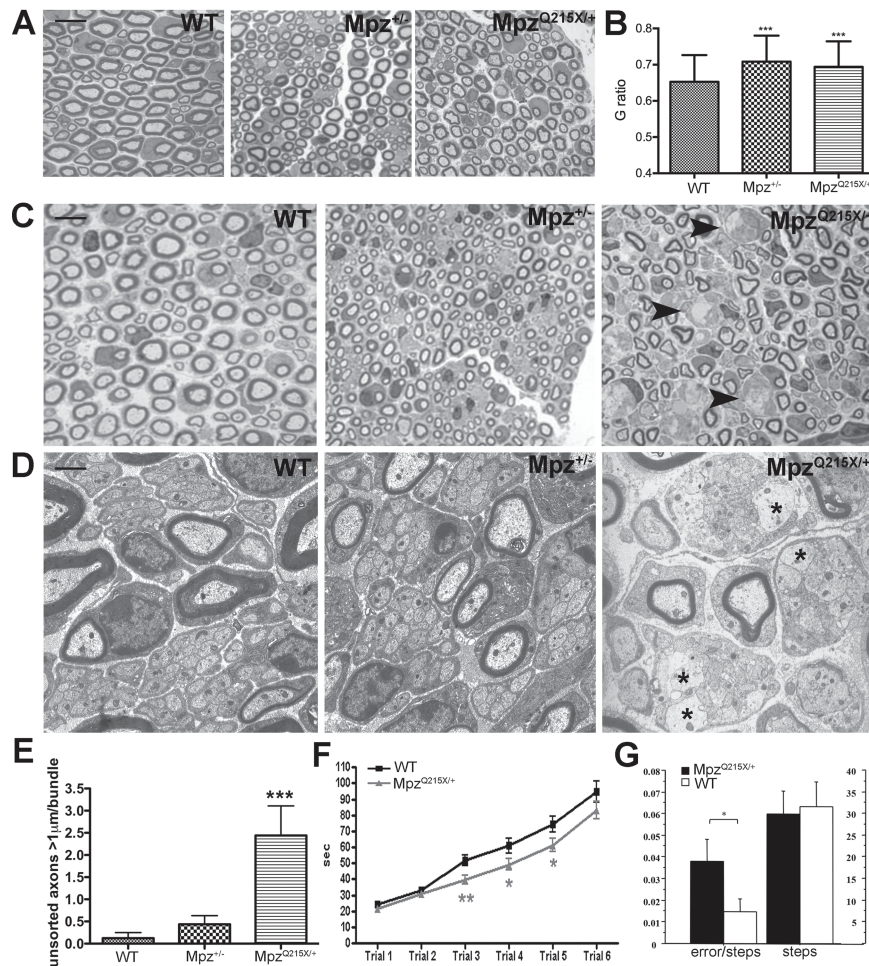
Figure 2. P0Q215X induces radial axonal sorting defects and neuropathy. (**A**) STSs of p28 SNs taken from $Mpz^{+/+}$, $Mpz^{+/-}$ and $Mpz^{Q215X/+}$ mice. Magnification, 100X; scale bar, 10 μm. (**B**) G-ratio quantifications of (A) (g-ratio $Mpz^{+/+}$ 0.65+/−0.002; g-ratio $Mpz^{+/-}$ 0.7+/−0.002; g-ratio $Mpz^{Q215X/+}$ 0.69+/−0.002); $n = 5$ mice/genotype, paired *t*-test, $P < 0.001$ versus WT. Error bars represent SEM). (**C**) STS of p11 SNs from $Mpz^{+/+}$, $Mpz^{+/-}$ and $Mpz^{Q215X/+}$ mice. Arrowheads indicate bundles of unsorted axons. (**D**) Electromicrographs of p11 SNs taken from $Mpz^{+/+}$, $Mpz^{+/-}$ and $Mpz^{Q215X/+}$ mice, showing details of bundles of unsorted axons (magnification, 20,000x; scale bar, 1 μm). (**E**) Number of unsorted axons (in direct contact with other axons, indicated by asterisks in the right panel) within the bundles, with a diameter > 1 μm ($n = 3$ mice/genotype, one-way ANOVA, Tukey test, $P < 0.001$ versus WT. Error bars represent SEM). (**F**) Rotarod analysis shows that $Mpz^{Q215X/+}$ mice at P11 ($n = 72$) remain on the accelerating cylinder for significantly less time than WT littermates ($n = 57$). Paired *t*-test, $*P < 0.05$ and $**P < 0.01$ versus WT. Error bars represent SEM. (**G**) Grid-walking test shows that $Mpz^{Q215X/+}$ mice at P15 ($n = 32$) had a number of errors as compared to WT littermate controls ($Mpz^{+/+}$; $n = 35$) with the same number of total steps. ANOVA genotype effect for errors F[1,65] = 8.33; $P = 0.005$. Error bars represent SEM.

P0Q215X does not induce ER stress and reaches the plasma membrane

Altered intracellular retention inducing ER stress has been previously associated and shown to play a crucial role in the pathogenesis of GOF *MPZ* mutations [15,17,27], prompting us to investigate whether P0Q215X induces ER stress and an unfolded protein response.

First, we generated $Mpz^{Q215X/Q215X}$, which only expresses the mutant protein, and determined whether P0Q215X was retained in the ER by performing co-staining with the ER marker KDEL on teased nerve fibers. We compared $Mpz^{Q215X/Q215X}$ to WT mice (Fig. 3A) and also to LoxP homozygous ($Mpz^{LoxP/LoxP}$) mice (Fig. 3B), which have a similar amount of *Mpz* expression. We could not detect P0Q215X in the ER (Fig. 3C), differently from P0S63del that we used as a positive control (Fig. 3D). Furthermore, mRNA levels of ER stress transcripts *BiP* and spliced *Xbp-1* were not significantly increased in $Mpz^{Q215X/Q215X}$ nerves, in contrast to nerves from mice carrying the P0S63del mutation, showing that the Q215X mutation does not induce ER stress (Fig. 3E). P0Q215X

was detected in the myelin of teased nerve fibers (Fig 3C), suggesting it can be normally trafficked. P0 forms tetramers before being targeted to myelin, and we tested whether P0Q215X is able to interact with its WT counterpart. We generated $Mpz^{Q215X/Q215X}$ mice expressing a myc-tagged P0WT (P0myc), allowing to perform an immunoprecipitation assay using an anti-myc antibody, in this setting specific to P0WT [6]. Western blot analysis of immunoprecipitates demonstrated pulldown of P0Q215X, supporting the interaction between P0Q215X and WTP0 (Supplementary Material, Fig. S2). Overall, this data shows that P0Q215X reach the plasma membrane, does not induce ER stress and can interact with P0WT.

P0Q215X is incorrectly trafficked to non-myelin plasma membranes

As the C-terminal domain has been shown to be important in targeting P0 to the membrane, we performed immunoelectron microscopy (IEM) on p10 $Mpz^{Q215X/Q215X}$ and $Mpz^{+/-}$ mice to
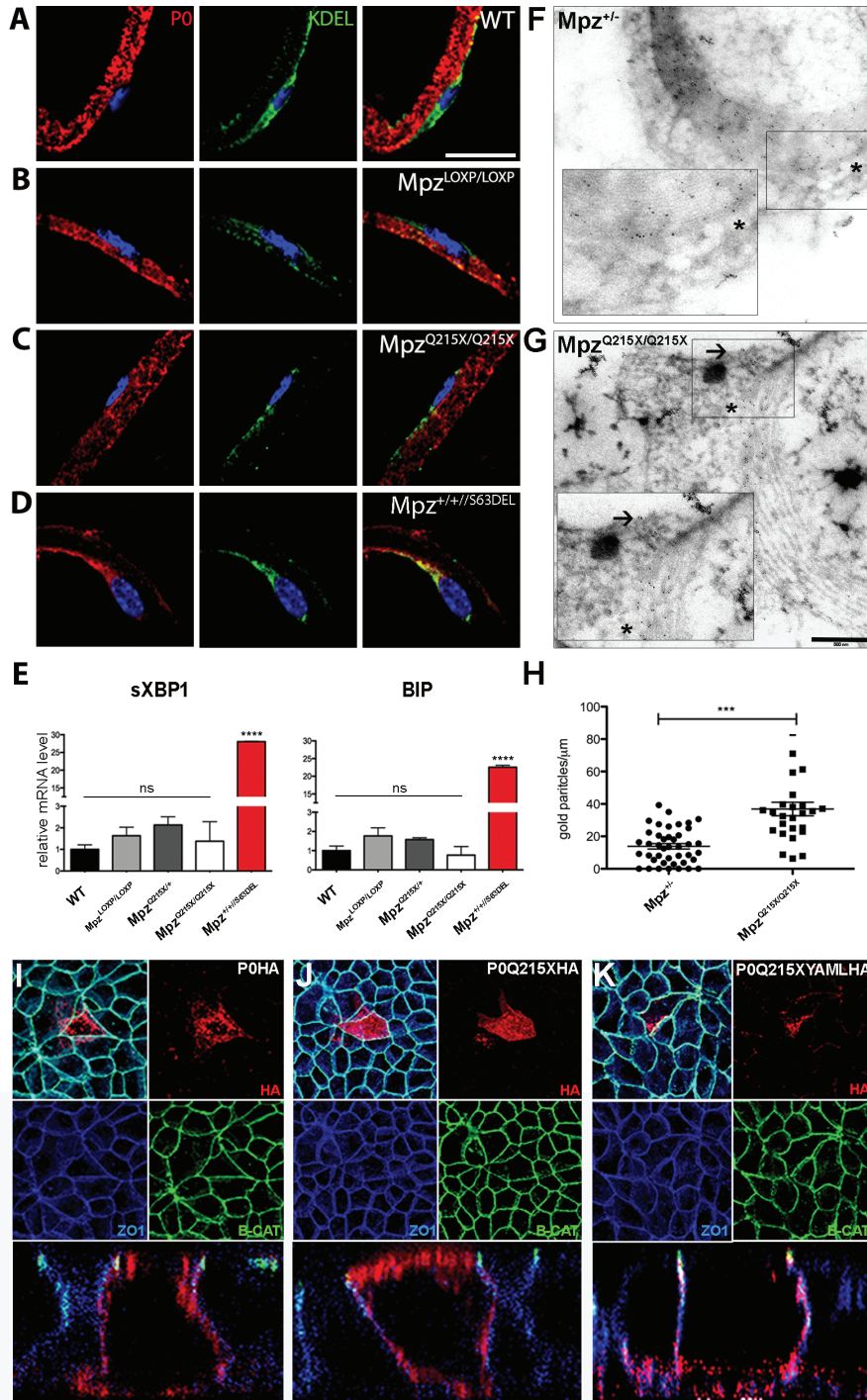
Figure 3. Lack of the YAML motif induces P0Q215X mistrafficking to non-myelin membrane. Immunohistochemistry on teased SN fibers from $Mpz^{Q215X/Q215X}$ (**C**) and $Mpz^{LoxP/LoxP}$ (**B**) mice show P0 ER retention in $Mpz^{+/+//P063del}$ mice (**D**) but not in $Mpz^{Q215X/Q215X}$ and WT controls (**A**). DAPI (blue), P0 (red), KDEL (green). Scale bar, 35 μm. (**E**) qPCR quantifications of XBP-1 and BiP levels show no significant changes in $Mpz^{Q215X/Q215X}$ ($n = 3$ mice/genotype; one-way ANOVA, Tukey's post-test. *P*-value versus WT ns and <0.001 (****). Error bars represent SEM. (**F, G**) IEM using anti-P0 Ab on $Mpz^{Q215X/Q215X}$ and $Mpz^{+/-}$ p10 SNs (scale bar, 500 nm). Asterisks show gold granules detected mainly in the compact myelin in both $Mpz^{Q215X/Q215X}$ and $Mpz^{+/-}$ p10 SNs, whereas arrows indicate P0 in non-myelin plasma membranes in $Mpz^{Q215X/Q215X}$ SNs. (**H**) Quantification of gold granules counted in non-myelin plasma membranes shows a statistically significant difference between $Mpz^{Q215X/Q215X}$ and $Mpz^{+/-}$ ($n = 3$ mice/genotype paired; *t*-test, $P < 0.0001$; error bars represent SEM). Transiently transfected MDCK cells expressing P0Q215X-YAML-HA, or P0Q215X-HA and P0WT-HA as controls, were stained for HA (red), ZO1 (blue, marker of basolateral surface) and Beta-catenin (green, marker of apical surface). Three independent replicates. (**I**) P0WT-HA is targeted to the basolateral surface of MDCK cells: in XZ confocal images, P0 immunostaining did not colocalize with apical marker Beta-catenin but was concentrated in basolateral membranes, which are immunostained for ZO1. (**J**) P0Q215X-HA was targeted to the apical surface and/or accumulated throughout the cell. (**K**) P0Q215X-YAML-HA is localized to the basolateral surface, similarly to P0WT-HA.
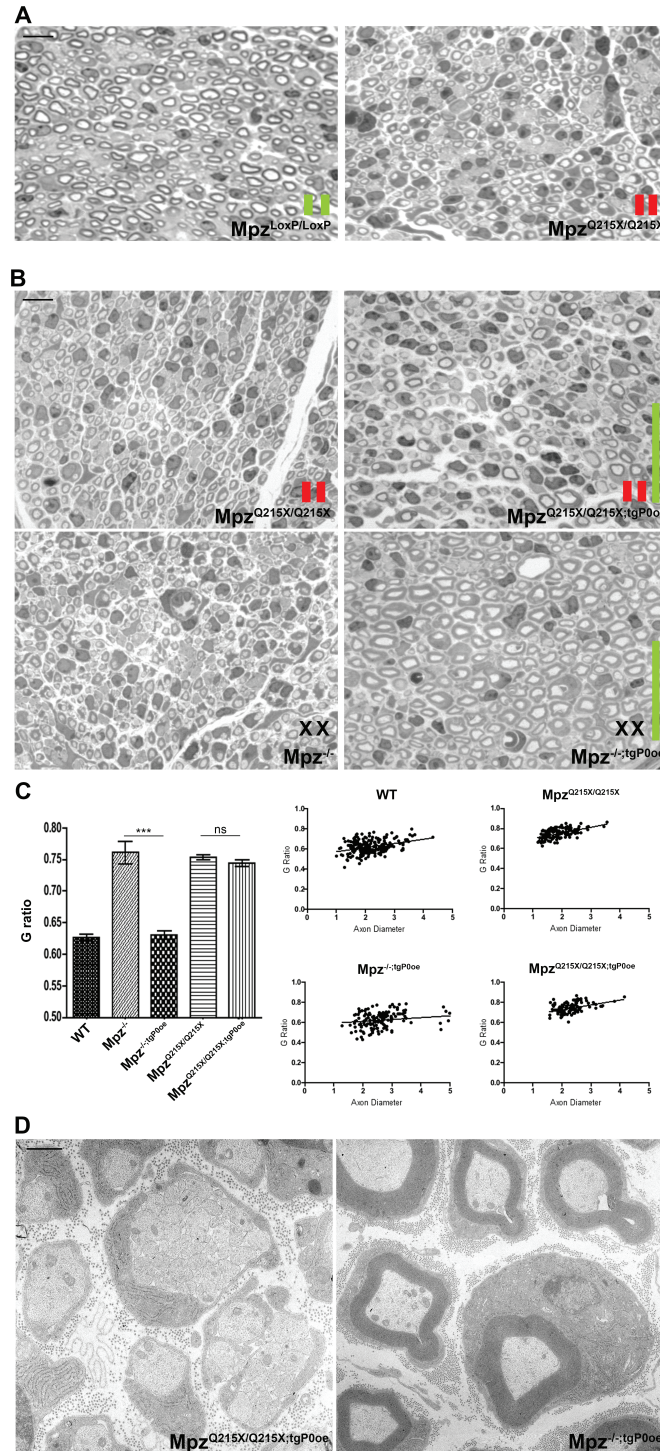
Figure 4. P0Q215X acts through gain of abnormal function. (**A**) STS of SNs from P10 $Mpz^{LoxP/LoxP}$ and $Mpz^{Q215X/Q215X}$ mice. $Mpz^{Q215X/Q215X}$ nerves are hypomyelinated when compared to $Mpz^{LoxP/LoxP}$ nerves (scale bar 10 μm). (**B**) STS of P10 nerves from $Mpz^{Q215X/Q215X}$ (upper panel, at left) and from $Mpz^{Q215X/Q215X}$ mice overexpressing P0WT ($Mpz^{Q215X/Q215X;tgP0oe}$, upper panel, at right); STS of P10 nerves from $Mpz^{-/-}$ (lower panel, at left) and $Mpz^{-/-}$ overexpressing P0WT ($Mpz^{-/-;tgP0oe}$, lower panel, at right); scale bar, 10 μm. Restoration of normal levels of P0wt is unable to rescue the hypomyelination in $Mpz^{Q215X/Q215X;tgP0oe}$ (upper panel, at right), whereas it does rescue the very severe hypomyelination in $Mpz^{-/-;tgP0oe}$ (lower panel, at right). In A and B, the red and the green bars indicate the expression of the WT (green) or mutated (red) alleles. (**C**) G ratio measured at P10 shows hypomyelination in $Mpz^{Q215X/Q215X;tgP0oe}$, whereas hypomyelination is rescued in $Mpz^{-/-;tgP0oe}$, where the G ratio is comparable to WT mice. G-ratio values: WT 0.63; $Mpz^{-/-}$ 0.76; $Mpz^{-/-;tgP0oe}$ 0.63; $Mpz^{Q215X/Q215X}$ 0.75; $Mpz^{Q215X/Q215X;tgP0oe}$ 0.74. $n = 5$ mice/genotype; paired *t*-test: $P < 0.0001$ $Mpz^{-/-}$ versus $Mpz^{-/-;tgP0oe}$ and P-value *ns* $Mpz^{Q215X/Q215X}$ versus $Mpz^{Q215X/Q215X;tgP0oe}$. Error bars represent SEM. (**D**) Electron micrographs confirms the rescue of myelin thickness in $Mpz^{-/-;tgP0oe}$ at P10 (right image), whereas hypomyelination and the sorting defects still remain in $Mpz^{Q215X/Q215X;tgP0oe}$ (left image). Scale bar, 1 μm.

assess this process. Gold granules indicate that P0 molecules are located primarily in the myelin sheath in $Mpz^{+/-}$ nerves (Fig. 3F and G, asterisks) and show that P0Q215X can still reach and can still be retained in compact myelin in $Mpz^{Q215X/Q215X}$ nerves, but interestingly, gold granules were also frequently detected outside of myelin in $Mpz^{Q215X/Q215X}$ nerves (Fig. 3G, arrows) suggesting that P0Q215X could be partially mistrafficked to non-myelin plasma membranes surrounding the SC body. Quantification of P0 showed an increase of the number of gold granules in non-myelin plasma membranes from $Mpz^{Q215X/Q215X}$ nerves, which is significantly higher than in the $Mpz^{+/-}$ controls (Fig. 3H). These data demonstrate that P0Q215X trafficking is altered *in vivo* with P0 being targeted to non-compact myelin membranes.

The YAML sequence in the cytoplasmic tail regulates P0 trafficking

P0Q215X lacks a YAML sequence in its C-terminal region, which has previously been implicated in myelin membrane targeting [12]. In order to address whether this determines the altered trafficking of P0Q215X, we used an *in vitro* assay where the YAML motif directs P0 trafficking to the basolateral surface of transfected and polarized MDCK cells [12]. We transfected MDCK cells with P0Q215X-HA or P0Q215X-YAML-HA and P0wt-HA as control, and stained the cells for hemagglutinin (HA), for Beta-catenin, a marker of the apical junction, and for ZO1, a marker of the basolateral surface. P0WT-HA was present at the basolateral surface of the cells (Fig. 3I), whereas the mutant P0Q215X-HA did not respect the basolateral distribution and was detected also at the apical surface (Fig. 3J). In contrast, the P0Q215X-YAML-HA construct was detected only at the basolateral surface of MDCK cells (Fig. 3K). These data show that YAML is sufficient to restore proper surface membrane targeting of P0Q215X, suggesting its deficiency determines the observed altered targeting of P0Q215X.

P0Q215X acts through a gain of abnormal function

Whether mutations act tough, gain- or loss-of-function is a crucial information as it has implications for therapeutic approaches. We reasoned that if the phenotype observed in $Mpz^{Q215X/Q215X}$ mice was due to hypomorphic P0 expression, i.e. a loss of function, then $Mpz^{LoxP/LoxP}$ should have a similar phenotype, whilst if GOF were involved, the phenotype should be aggravated in a dose-dependent manner. To therefore test whether Q215X induces disease by a dosage-dependent GOF, we first generated $Mpz^{Q215X/Q215X}$ mice and we compared myelination to that of $Mpz^{LoxP/LoxP}$ mice, that express equivalent levels of wt *Mpz*. Whilst the reduced amount of WT *Mpz* expressed in $Mpz^{LoxP/LoxP}$ mice (∼20% of normal) was sufficient for myelination in SNs at P10, $Mpz^{Q215X/Q215X}$ animals (also expressing ∼20% of normal) manifested a very severe hypomyelination at this age (Fig. 4A). To further eliminate the confounding element of LOF in $Mpz^{Q215X/Q215X}$ mice, we crossed $Mpz^{Q215X/Q215X}$ mice with a P0 overexpressor transgenic mouse line ($Mpz^{+/+;tgP0oe}$) [26]. The $Mpz^{+/+;tgP0oe}$ mice express *Mpz* wt at 80% on top of normal (where normal refers to two *Mpz* wt alleles) and were previously demonstrated to fully rescue the P0 null phenotype at P28 [26]. We compared $Mpz^{Q215X/Q215X;tgP0oe}$ mice to $Mpz^{-/-;tgP0oe}$ mice at P10. Consistent with previous results STS from $Mpz^{-/-;tgP0oe}$ SNs show normal myelination (Fig. 4B) with a G-ratio similar to WT (Fig. 4C; G-ratio values: WT 0.63; P0ko 0.76; P0ko//P0oe 0.63). Electron microscopic (EM) analysis confirmed the presence of normally compacted, thick myelin sheaths in these specimens (Fig. 4D)—demonstrating that the P0oe transgene is able to

rescue the $Mpz^{-/-}$ phenotype also at P10. In contrast, STS from $Mpz^{Q215X/Q215X;tgP0oe}$ SNs showed abnormally thin myelin (Fig. 4B). EM analysis showed bundles of unsorted axons as previously described and, most remarkably, very severe hypomyelination in SN (Fig. 4D). P0WT was unable to induce an amelioration when compared to $Mpz^{Q215X/Q215X}$, and the G-ratio was not significantly different (Fig. 4C; G-ratio values: Q215X/Q215X 0.75; Q215X/Q215X//P0oe 0.74). These data conclusively demonstrate that Q215X causes the myelin phenotype by a dose-dependent GOF mechanism.

Discussion

We have generated a novel mouse model for CH induced by a nonsense *MPZ* mutation. We first show, using patient tissue, that the mutation escapes NMD and is expressed similarly to its WT counterpart. In both our mutant mice and in control lines, where a WT-Mpz allele was inserted and therefore carry a LoxP site, *Mpz* expression is reduced due to the presence of the LoxP sites in intron 5, and, as expected, the premature stop codon gives rise to a truncated protein in mice. This provides a model system where a very aggressive mutation is expressed at more limited levels, potentially allowing us to discern more subtle phenotypes. Recently developed and now widely used approaches with CRISPR-Cas9 would be predicted to not influence the expression levels and we would therefore expect a more severe phenotype to develop. Interestingly, protein levels appear lower compared to WT LoxP alleles, suggesting reduced protein stability. The mutant heterozygous mice, in keeping with the reduced expression of mutant *Mpz*, develop a phenotype that is less severe than that of patients, but nonetheless show hypomyelination. We were also able to identify a novel defect in axonal radial sorting during myelination at P10, which is intriguing, as defects at the axonal sorting stage are compatible with the early-onset developmental phenotype observed in patients.

Normally P0 is synthesized in the ER, glycosylated, assembled as tetramers and then targeted to the myelin membrane, and early stages of this process have been shown to be altered in other disease-causing mutations [15,17,27]. We therefore used a combination of molecular mouse tools, biochemical, confocal microscopy and IEM approaches to investigate P0Q215X maturation, and show that P0Q215X is able to correctly mature, interact with its WT counterpart and be trafficked to the membrane. No ER stress is induced, clearly differentiating the mechanism of action from other *MPZ* mutations causative of CMT or CH that we previously characterized in mice [15,17,27].

As one of the known functions for P0 cytoplasmic domain, which is truncated in P0Q215X, is to target the protein to myelin [12], we analyzed in detail the membrane targeting of the protein, and found that Q215X was increasingly misdirected to non-myelin plasma membranes. We then used an *in vitro* assay to show that reinsertion of the YAML in the cytoplasmic domain is able to rescue the trafficking of P0Q215X. Interestingly, even WT P0, if overexpressed at very high levels, is mislocalized at the abaxonal membrane and mesaxon, causing CH due to radial sorting defects and amyelination. The latter is probably due to a gain of normal P0 function that causes homophilic P0 adhesion between apposed mesaxonal membranes [26,29]. These findings have important implications as, potentially, the targeting of an adhesive protein such as P0 to incorrect membrane domains may contribute also to the altered axonal radial sorting process, where SC membranes need to extend between and isolate axons.

The mistargeting of P0 protein is compatible in principle with both gain- and loss-of-function mechanisms. Dissecting the contribution of gain and loss of function is extremely important, especially in light of the recent increase in genetic therapy approaches, where for example PMP22 is targeted for reduction by means of antisense oligonucleotides in a CMT1A [30]. Our findings of an axonal sorting phenotype being present only in $Mpz^{Q215X/+}$ and not in $Mpz^{+/-}$ mice suggested= a GOF and in order to conclusively address this issue, we increased the dosage of mutant P0Q215X by breeding mice to homozygosity and then asked whether supplementation of P0WT protein would rescue the phenotype. Homozygous mice showed a very severe phenotype, but P0WT supplementation, which was able to rescue the full loss of P0 in $Mpz^{-/-}$ mice, was unable to correct the P0Q215X toxicity, strongly indicating GOF as the main mode of action.

The fact that different *MPZ* mutations have very distinct mechanisms of action, but the commonality of a GOF mechanism, has strong therapeutic implications. It makes it unlikely to develop a therapeutic approach targeting such a wide range of biological processes (e.g. altered membrane targeting, ER stress etc.), but supports a genetic therapeutic approach based on allele-specific knock down. Although, currently, gene silencing is being pursued only in conditions where the same mutation is present in a wide number of patients (e.g. CMT1A), future developments may use common polymorphism to develop an array of silencing tools. This will allow for a silencing approach to be applied to less frequent mutations such *MPZ*.

Materials and Methods

All materials and methods can be found in the Supplementary Materials.

Acknowledgements

Funding

References

1. Archelos, J.J., Roggenbuck, K., Schneider-Schaulies, J., Linington, C., Toyka, K.V. and Hartung, H.P. (1993) Production and characterization of monoclonal antibodies to the extracellular domain of P0. *J. Neurosci. Res.*, **35**, 46–53.

2. Baets, J., Deconinck, T., De Vriendt, E., Zimoń, M., Yperzeele, L., Van Hoorenbeeck, K., Peeters, K., Spiegel, R., Parman, Y., Ceulemans, B. *et al.* (2011) Genetic spectrum of hereditary neuropathies with onset in the first year of life. *Brain*, **134**, 2664–2676.

3. D'Urso, D., Brophy, P.J., Staugaitis, S.M., Gillespie, C.S., Frey, A.B., Stempak, J.G. and Colman, D.R. (1990) Protein zero of peripheral nerve myelin: biosynthesis, membrane insertion, and evidence for homotypic interaction. *Neuron*, **4**, 449–460.

4. Feltri, M.L., D'antonio, M., Quattrini, A., Numerato, R., Arona, M., Previtali, S., Chiu, S.Y., Messing, A. and Wrabetz, L. (1999) A novel P0 glycoprotein transgene activates expression of lacZ in myelin-forming Schwann cells. *Eur. J. Neurosci.*, **11**, 1577–1586.

5. Filbin, M.T., Walsh, F.S., Trapp, B.D., Pizzey, J.A. and Tennekoon, G.I. (1990) Role of myelin P0 protein as a homophilic adhesion molecule. *Nature*, **344**, 871–872.

6. Fratta, P., Saveri, P., Zambroni, D., Ferri, C., Tinelli, E., Messing, A., D'Antonio, M., Feltri, M.L. and Wrabetz, L. (2011) P0S63del impedes the arrival of wild-type P0 glycoprotein to myelin in CMT1B mice. *Hum. Mol. Genet.*, **20**, 2081–2090.

7. Giese, K.P., Martini, R., Lemke, G., Soriano, P. and Schachner, M. (1992) Mouse P0 gene disruption leads to hypomyelination, abnormal expression of recognition molecules, and degeneration of myelin and axons. *Cell*, **71**, 565–576.

8. Greenfield, S., Brostoff, S., Eylar, E.H. and Morell, P. (1973) Protein composition of myelin of the peripheral nervous system. *J. Neurochem.*, **20**, 1207–1216.

9. Ho, S.N., Hunt, H.D., Horton, R.M., Pullen, J.K. and Pease, L.R. (1989) Site-directed mutagenesis by overlap extension using the polymerase chain reaction. *Gene*, **77**, 51–59.

10. Inoue, K., Shilo, K., Boerkoel, C.F., Crowe, C., Sawady, J., Lupsky, J.R. and Agamanolis, D.P. (2002) Congenital hypomyelinating neuropathy, central dysmyelination, and Waardenburg-Hirschsprung disease: phenotypes linked by SOX10 mutation. *Ann. Neurol.*, **52**, 836–842.

11. Inoue, K., Khajavi, M., Ohyama, T., Hirabayashi, S., Wilson, J., Reggin, J.D., Mancias, P., Butler, I.J., Wilkinson, M.F., Wegner, M. and Lupski, J.R. (2004) Molecular mechanism for distinct neurological phenotypes conveyed by allelic truncating mutations. *Nat. Genet.*, **36**, 361–369.

12. Kidd, G.J., Yadav, V.K., Huang, P., Brand, S.L., Low, S.H., Weimbs, T. and Trapp, B.D. (2006) A dual tyrosine-leucine motif mediates myelin protein P0 targeting in MDCK cells. *Glia*, **54**, 135–145.

13. Mandich, P., Mancardi, G.L., Varese, A., Soriani, S., Di Maria, E., Bellone, E., Bado, M., Gross, L., Windebank, A.J., Ajmar, F. and Schenone, A. (1999) Congenital hypomyelination due to myelin protein zero Q215X mutation. *Ann. Neurol.*, **45**, 676–678.

14. Martini, R., Zielasek, J., Toyka, K.V., Giese, K.P. and Schachner, M. (1995) Protein zero (P0)-deficient mice show myelin degeneration in peripheral nerves characteristic of inherited human neuropathies. *Nat. Genet.*, **11**, 281–286.

15. Pennuto, M., Tinelli, E., Malaguti, M., Del Carro, U., D'Antonio, M., Ron, D., Quattrini, A., Feltri, M.L. and Wrabetz, L. (2008) Ablation of the UPR-mediator CHOP restores motor function and reduces demyelination in Charcot-Marie-Tooth 1B mice. *Neuron*, **57**, 393–405.

16. Quattrini, A., Previtali, S., Feltri, M.L., Canal, N., Nemni, R. and Wrabetz, L. (1996) Beta 4 integrin and other Schwann cell markers in axonal neuropathy. *Glia*, **17**, 294–306.

17. Saporta, M.A., Shy, B.R., Patzko, A., Bai, Y., Pennuto, M., Ferri, C., Tinelli, E., Saveri, P., Kirschener, D., Crowther, M. *et al.* (2012) MpzR98C arrests Schwann cell development in a mouse model of early-onset Charcot-Marie-Tooth disease type 1B. *Brain*, **135**, 2032–2047.

18. Sanmaneechai, O., Feely, S., Scherer, S.S., Herrmann, D.N., Burns, J., Muntoni, F., Li, J., Siskind, C.E., Day, J.W., Laura, M. *et al.* (2015) Genotype-phenotype characteristics and baseline natural history of heritable neuropathies caused by mutations in the MPZ gene. *Brain*, **138**, 3180–3192.

19. Schwenk, F., Baron, U. and Rajewsky, K. (1995) A cre-transgenic mouse strain for the ubiquitous deletion of loxP-flanked gene segments including deletion in germ cells. *Nucleic Acids Res.*, **23**, 5080–5081.

20. Shapiro, L., Doyle, J.P., Hensley, P., Colman, D.R. and Hendrickson, W.A. (1996) Crystal structure of the extracellular domain from P0, the major structural protein of peripheral nerve myelin. *Neuron*, **17**, 435–449.

21. Shy, M.E., Jani, A., Krajewski, K., Grandis, M., Lewis, R.A., Li, J., Shy, R.R., Balsamo, J., Lilien, J., Garbern, J.Y. and Kamholz, J. (2004) Phenotypic clustering in MPZ mutations. *Brain*, **127**, 371–384.

22. Trapp, B.D., Andrews, S.B., Cootauco, C. and Quarles, R.H. (1989) The myelin-associated glycoprotein is enriched in multivesicular bodies and periaxonal membranes of actively myelinating oligodendrocytes. *J. Cell. Biol.*, **109**, 2417–2426.

23. Warner, L.E., Hilz, M.J., Appel, S.H., Killian, J.M., Kolodry, E.H., Karpati, G., Carpenter, S., Watters, G.V., Wheeler, C., Witt, D. *et al.* (1996) Clinical phenotypes of different MPZ (P0) mutations may include Charcot-Marie-Tooth type 1B, Dejerine-Sottas, and congenital hypomyelination. *Neuron*, **17**, 451–460.

24. Wong, M.H. and Filbin, M.T. (1994) The cytoplasmic domain of the myelin P0 protein influences the adhesive interactions of its extracellular domain. *J. Cell. Biol.*, **126**, 1089–1097.

25. Wong, M.H. and Filbin, M.T. (1996) Dominant-negative effect on adhesion by myelinPo protein truncated in its cytoplasmic domain. *J. Cell. Biol.*, **134**, 1531–1541.

26. Wrabetz, L., Feltri, M.L., Quattrini, A., Imperiale, D., Previtali, S., D'Antonio, M., Martini, R., Yin, X., Trapp, B.D., Zhou, L., Chiu, S.Y. and Messing, A. (2000) P(0) glycoprotein overexpression causes congenital hypomyelination of peripheral nerves. *J. Cell. Biol.*, **148**, 1021–1034.

27. Wrabetz, L., D'Antonio, M., Pennuto, M., Dati, G., Tinelli, E., Fratta, P., Previtali, S., Imperiale, D., Zielasek, J., Toyka, K. *et al.* (2006) Different intracellular pathomechanisms produce diverse myelin protein zero neuropathies in transgenic mice. *J. Neurosci.*, **26**, 2358–2368.

28. Xu, W., Shy, M., Kamholz, J., Elferink, L., Xu, G., Lilien, J. and Balsamo, J. (2001) Mutations in the cytoplasmic domain of P0 reveal a role for PKC-mediated phosphorylation in adhesion and myelination. *J. Cell Biol.*, **155**, 439–446.

29. Yin, X., Kidd, G.J., Wrabetz, L., Feltri, M.L., Messing, A. and Trapp, B.D. (2000) Schwann cell myelination requires timely and precise targeting of P0 protein. *J. Cell Biol.*, **148**, 1009–1020.

30. Zhao, H.T., Damle, S., Ikeda-Lee, K., Kuntz, S., Li, J., Mohan, A., Kim, A., Hung, G., Scheideler, M.A., Scherer, S.S. *et al.* (2018) PMP22 antisense oligonucleotides reverse Charcot-Marie-Tooth disease type 1A features in rodent models. *J. Clin. Invest.*, **128**, 359–368.